JOURNAL OF GEOPHYSICAL RESEARCH, VOL. 113, D20125, doi:10.1029/2008JD010294, 2008

Simultaneous remote electric and magnetic field measurements of lightning continuing currents

Manus Ross,[1,2] Steven A. Cummer,[1] Thomas K. Nielsen,[3] and Yongming Zhang[3]

Received 18 April 2008; revised 20 August 2008; accepted 4 September 2008; published 31 October 2008.

[1] Remote detection and measurement of the slowly varying continuing current that follows some lightning return strokes is difficult. Slow changes in quasi-static electric fields have been most frequently used to remotely measure continuing current. Because of the rapid attenuation of dipole electric fields with distance, though, the range over which the current will produce a measurable signature in the field is limited. Here we report the analysis of continuing current signatures observed in both the quasi-static electric and magnetic fields from four lightning strokes that were recorded from a range of 52 to 96 km at a measurement site near Fort Collins, Colorado on 15 July 2005. Electro- and magnetostatic analyses show that the distinct magnetic and electric field signatures are produced by the continuing current and the associated net charge transfer, respectively. The measurements confirm that the quasi-static magnetic fields that follow some return strokes are signatures of continuing current. Using realistic noise estimates based on our measurements, we also show that modest to large continuing currents can be reliably detected and measured from long ranges (more than 1000 km for 1 kA) using quasi-static magnetic field signatures.

Citation: Ross, M., S. A. Cummer, T. K. Nielsen, and Y. Zhang (2008), Simultaneous remote electric and magnetic field measurements of lightning continuing currents, *J. Geophys. Res.*, *113*, D20125, doi:10.1029/2008JD010294.

1. Introduction

[2] Continuing current is the slowly varying lightning current that immediately follows a return stroke and typically lasts for tens to hundreds of milliseconds [*Rakov and Uman*, 2003]. Continuing current is of practical interest because it is thought to be responsible for much of the serious damage due to lightning, including forest fires [*Fuquay et al.*, 1967], burned holes in the metal skins of aircraft [*Fisher and Plumer*, 1977], and certain kinds of power line damage [*Nakahori et al.*, 1982]. Scientifically, continuing currents are also of interest because relatively little is known about the lightning physics and meteorology responsible for them. Work has been done to investigate the cause of continuing current; studies by *Shindo and Uman* [1989] have shown that when a series of lightning strokes occurred, there was a fundamental difference between the way that the first strokes and subsequent strokes terminate in the cloud, and this difference may enable or cause a continuing current. *Brook et al.* [1962] have shown that the charge transferred by return strokes that initiate long continuing current is smaller than for strokes that do not.

[3] Continuing current measurements can be most precisely made by direct measurements of triggered lightning or lightning that strikes an instrumented tower [e.g., *Fisher et al.*, 1993]. In the absence of such measurements, continuing currents are most often detected by their signature in measured ground-level static or quasi-static electric fields. This signature is a slow increase in the magnitude of the electric field change because of the steady charge transfer in the continuing current. This signature is usually easily detectable up to several tens of km from the lightning, but because of the r^{-3} field decay with distance from the electric dipole formed by the lightning charge and its image in the ground, the range of continuing current detectability through electric fields is limited. Provided the range to the lightning is known, the continuing current amplitude can be estimated from the measured electric field through comparison with a simple analytical calculation that includes the source charge and all of its images in the ground and the ionosphere. This calculation becomes increasingly sensitive to the assumed ionospheric altitude at longer ranges. The rapid field decay with distance also means that the range to the center of charge removal must be known precisely, and return stroke locations can be offset from the charge removal centroid on the order of kilometers. This latter uncertainty can be reduced through multi-point measurements [*Krehbiel et al.*, 1979]. However the uncertainties in the charge-centroid-to-sensor range and the effective ionospheric height can introduce significant errors in continuing current measurements based on electric fields.

[4] Continuing currents also produce a quasi-static magnetic field signature [*Williams and Brook*, 1963] that can be measured remotely with sufficiently sensitive instruments. *Cummer and Füllekrug* [2001] showed that slowly varying

[1]Electrical and Computer Engineering Department, Duke University, Durham, North Carolina, USA.
[2]Now at MTS Systems Corporation, Cary, North Carolina, USA.
[3]QUASAR Federal Systems, San Diego, California, USA.

0148-0227/08/2008JD010294$09.00

magnetic field signatures with amplitudes of a few tens of pT that followed some sprite producing lightning strokes were consistent with unusually large continuing currents on the order of several and even tens of kA. The signatures were recorded more than 1000 km from the lightning, demonstrating a long detection range for these large continuing currents that is consistent with the much slower r^{-1} magnetic field decay with distance indicated by magnetostatic calculations for ranges where the image currents in the ionosphere are important. However the connection of these long-range quasi-magnetostatic signatures with continuing current has not until now been confirmed with independent measurements.

[5] Here we analyze simultaneously measured quasi-static electric and magnetic fields from lightning to demonstrate that the two independent methods yield the same continuing current charge transfer, thereby validating the magnetic field measurement and analysis technique. From these measurements we realistically estimate the minimum detectable electric and magnetic field signatures and assess the relative sensitivity of these two methods as a function of range.

2. Instruments and Data

[6] From 26 June to 15 August 2005, an electric field sensor and two orthogonal magnetic field induction coil sensors were placed at a field station in Ft. Collins, CO (latitude 40.67°N, longitude −104.94°E) to measure the vertical electric field and horizontal magnetic field produced by lightning at both short and long ranges. The electromagnetic sensors were designed and built by Quasar Federal Systems, Inc. and were designed for sensitivity at low frequencies in a compact package. The magnetic field sensing element is a coil of approximately 2 cm diameter and 45 cm length. The electric field sensor operates by measuring the free-space potential difference between two circular metal plates of approximately 5 cm diameter separated by approximately 20 cm. In our application the sensor was oriented with a vertical separation between the plates to measure the vertical field component and was mounted approximately 30 cm above locally flat ground.

[7] The magnetic field sensors have a flat response with −3 dB frequencies at 3.0 Hz and 20 kHz, and the electric field sensor has a flat response between −3 dB frequencies of 2.3 Hz and 25 kHz (including anti-aliasing filters). The three signals were sampled continuously at 100 kHz with GPS-based absolute timing to ensure the accurate identification of individual lightning strokes from National Lightning Detection Network (NLDN) data [*Cummins et al.*, 1998].

[8] Absolute sensor calibration is critical for this analysis. A pre-campaign cross calibration based on outdoor field measurements between the Quasar magnetic field sensors and two different sets of magnetic sensors deployed at Duke University indicated that the absolute magnetic field calibration uncertainties are on the order of 5%. Care was taken not to use any magnetic materials in the sensor installation in Colorado, and consequently the prior calibration should remain valid. Electric field sensors are highly sensitive to environment and installation however. To calibrate the electric sensor we relied on the fact that for distant lightning strokes and frequencies above approximately 2 kHz so that the propagation distance is at least several wavelengths, $E_z = cB_\phi$, where E_z is the vertical electric field, B_ϕ is the horizontal azimuthal magnetic field, and c is the speed of light in a vacuum. Consequently we calibrated the E sensor through a frequency domain comparison between vertical E and the azimuthal B fields using several high signal to noise ratio sferics originating from more than 1000 km from the sensor across the 5 kHz to 15 kHz bandwidth. This frequency range was chosen to encompass most of the signal energy and be safely above the frequencies where $E_z = cB_\phi$ is not valid.

[9] The low end frequency cutoffs also play an important role in the presented analysis. The 2.3 Hz E sensor cutoff was measured in the field from the exponential decay of several signals from nearby lightning strokes that were confirmed using high speed video not to contain continuing current, while the 3.0 Hz B sensor cutoff was measured in the lab calibration and through a cross comparison with the EMI BF-4 coils at Duke University, which have a flat frequency response significantly below 1 Hz. These low frequency cutoffs mean that the fields produced by a constant continuing current, namely a constant magnetic field and a linearly increasing electric field, will not be measured as such. The measured magnetic field will exponentially decay to zero and the measured electric field slope will exponentially decay to zero (and thus the electric field to a constant value) with time constants corresponding to the low frequency cutoff frequencies—68 ms for the E sensor and 53 ms for the B sensors.

[10] In light of the impact of the low frequency sensor response, we limit our analysis to the signals between 10 and 40 ms after the lightning stroke to minimize the decay of the continuing current signatures. The signal decay in this period will reduce the total continuing current charge moment change by 24% for the E sensor and 30% for the B sensors, and consequently the measured charges reported below are too low by approximately these factors. Because the time constants are close to each other, the effects on the measurements from each sensor are nearly identical. This modest and equal reduction of the charge transfers measured with each sensor does not impact the primary aim of this work, which is to show that the electric and magnetic field signatures are quantitatively consistent with the same total continuing current.

[11] In postprocessing, the two magnetic field signals were combined as vectors to give the magnetic field component transverse to the propagation path. This B_ϕ is the azimuthal component in a coordinate system centered at the lightning and is the component produced by a quasi-static vertical line current and thus is the component that contains the quasi-static magnetic field signature of continuing current. We define the vertical electric field E_z as positive upward to be consistent with a right handed coordinate system centered at the lightning. In both the B_ϕ and E_z signals, power line noise is removed in post processing by subtraction of a synthesized noise-only waveform.

[12] Figure 1 shows the denoised but full bandwidth azimuthal magnetic (B_ϕ) and vertical electric (E_z) fields of a lightning stroke that contains a clear continuing current signature in both fields. Note that because all of the lightning strokes analyzed here are positive polarity, in this

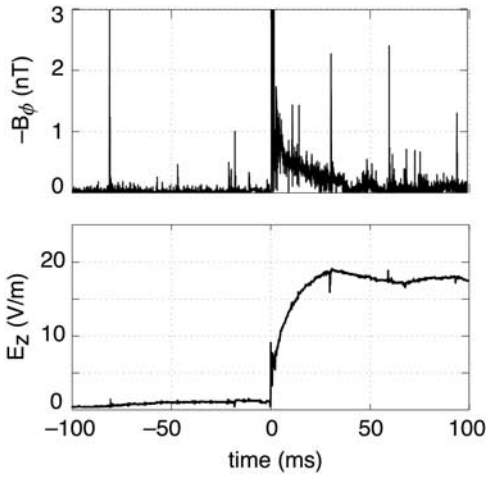

Figure 1. Unfiltered B_ϕ and E_z for a stroke containing a continuing current signature in both fields, namely a slow increase in E and an elevated B following the return stroke.

figure and those that follow, the displayed magnetic field waveform is the inverted azimuthal magnetic field $-B_\phi$ (which is labeled on each axis) so that the signal appears with a positive polarity. The plots illustrate a typical case for the class of lightning strokes discussed in this analysis. The sharp pulses in both signals at $t = 0$ ms correspond to the return stroke. For approximately 40 ms following the return stroke, the E_z signal shows a slowly increasing amplitude, while the B_ϕ signal shows an elevated non-zero amplitude. This slow E variation is well known to be the signature of a continuing current and is produced by the steadily increasing charge imbalance produced by the continuing current. This signature can also be produced by overhead in-cloud processes, but this lightning stroke was NLDN-geolocated at a range of 71 km from the sensor and thus it is almost certain that this is a continuing current signature. The elevated B signal following the return stroke is the corresponding magnetic field signature of a continuing current, in which the physical current and its images in the ionosphere and ground produce a field that is linearly proportional to the instantaneous current [*Cummer and Füllekrug*, 2001]. Our aim here is to show that these two signatures are quantitatively consistent with a single continuing current magnitude.

[13] NLDN data were used to identify lightning strokes that possessed a continuing current signature in both the magnetic and electric fields. Since this investigation requires an identifiable continuing current signature in both the electric and magnetic fields, and the electric field decays at a rate proportional to r^{-3}, we only considered lightning strokes that were within 100 km of our sensors. There were 8 lightning-producing storms with a total of 338 strokes that were within 100 km of our sensors during the campaign period between 26 June and 15 August 2005. We further limited the analysis to events that occurred at night, for which we could reasonably assume that the effective ionosphere height, a parameter that enters the quantitative analysis, is not time varying. This left 3 storms that produced a total of 116 lightning strokes. The first storm took place between 0200 UT and 0400 UT on 15 July 2005 and produced 69 strokes that fit the aforementioned criteria; the second storm took place between 0415 UT and 0515 UT on 1 August 2005 and produced 9 strokes; and the third storm was active between 0315 UT and 0415 UT on 3 July 2005 and produced 38 strokes.

[14] The recorded E_z and B_ϕ data for these 116 strokes were then analyzed using a combination of automatic and manual processing to determine whether a detectable continuing current signature was present in the magnetic field. The end result was 4 lightning strokes with very clear continuing current signatures in both the B_ϕ and E_z fields. All of them are positive CG strokes. This modest number is sufficient to demonstrate the consistency of the magnetic and electric field signatures of continuing current.

3. Analysis Method and Effective Ionospheric Height

[15] These data are quantitatively interpreted using a static field analytical approximation in which the charge is assumed to be removed from a single point in the cloud. This is a reasonable approximation for measurements made a significant distance from the source (50–100 km in our events), but do not adequately describe the fields close to the lightning stroke where this point approximation is violated. The Biot–Savart law and the method of images give the ground-level azimuthal magnetic field $B_\phi(t)$ at a distance r from a slowly varying lightning current $i(t)$ with channel length ℓ directly above a conducting surface and also with a second conducting surface (the ionosphere) located at height h_i, namely

$$B_\phi(t) = \frac{\mu_0 i(t)\ell}{2\pi}\left[\frac{1}{r\sqrt{r^2+\ell^2}} + \sum_{m=1}^{\infty}\frac{2r}{\left[r^2+(2mh_i)^2\right]^{\frac{3}{2}}}\right], \quad (1)$$

where it has been assumed that $\ell \ll \sqrt{r^2+(2mh_i)^2}$ to simplify the contributions from the image currents. For short distances from the source ($r \ll h_i$) the magnetic field decays as r^{-2} with distance because the first term in the brackets dominates. However, for longer distances where $r \gtrsim h_i$, the sum of the fields from the infinite series of images approximates the fields that would be produced by a continuous and infinite line current. In this range the magnetic field decays with distance as r^{-1}.

[16] Similarly, Coulomb's law and the method of images give the ground-level vertical electric field at a distance r from a slowly varying charge $q(t)$ at a distance ℓ directly above a conducting surface and including a second conducting surface at height h_i, namely

$$E_z(t) = \frac{q(t)\ell}{2\pi\epsilon_0}\left[\frac{1}{(r^2+\ell^2)^{\frac{3}{2}}} + \sum_{m=1}^{\infty}\frac{2mh_i+\ell}{\left[\ell(2mh_i+\ell)^2+r^2\right]^{\frac{3}{2}}} - \frac{2mh_i-\ell}{\ell\left[(2mh_i-\ell)^2+r^2\right]^{\frac{3}{2}}}\right]. \quad (2)$$

In both equations (1) and (2) m is an integer that enumerates the pair of image currents or electric dipoles a distance of $\pm 2h_i$ above and below the ground plane. These expressions have purposely been written in terms of current moment $I\ell$

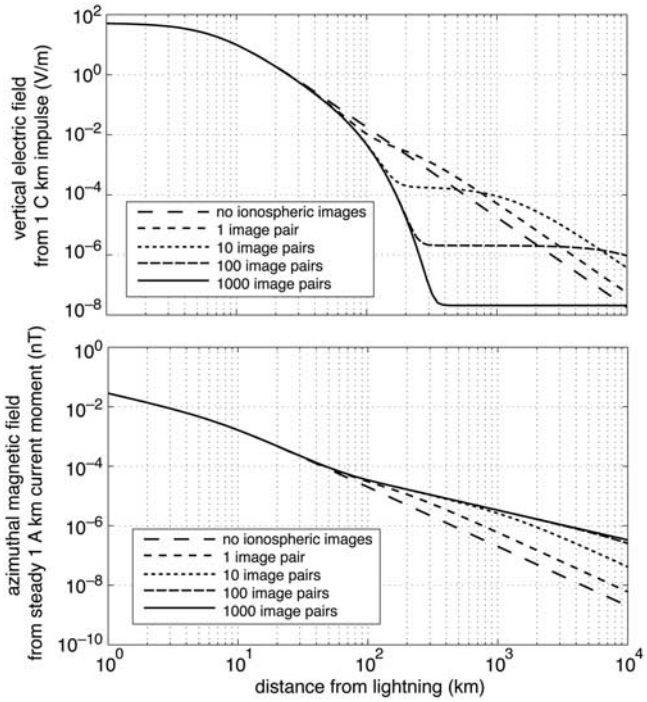

Figure 2. Computed electrostatic (top) and magnetostatic (bottom) fields versus distance for different numbers of ionospheric image pairs.

and charge moment $Q\ell$ because for distances $r \gg \ell$, the scaling constants inside the brackets in both of these expressions are largely independent of ℓ, and consequently the current and charge moments are the quantities that can be inferred from distant magnetic and electric field measurements.

[17] To give a sense of the importance of the ionospheric images in the static fields, the top panel of Figure 2 shows the electrostatic field versus distance produced by an impulsive 1 C km charge moment change (assuming ℓ = 7 km and h_i = 60 *km* as a function of the number of image pairs m in the summation of equation (2). The ionospheric images are of increasing importance with increasing range, changing the distance dependence from r^{-3} to exponential decay, and they reduce the overall vertical electric field magnitude. The bottom panel of Figure 2 shows the same but for the magnetostatic field produced by a steady 1 A km current moment. In this case the ionospheric images increase the overall azimuthal magnetic field and change the distance decay from r^{-2} to r^{-1}. For strokes less than 100 km away from the sensors, it is evident that 100 image pairs in the above summations are sufficient to achieve practical convergence. Note that these are quasi-static fields for which the wavelength approaches infinity and thus the radiation field relationship $E_z = cB_\phi$ is never valid.

[18] The effective ionospheric height (h_i) is an important parameter in determining both B_ϕ and E_z. Note that the value of h_i relevant for quasi-static field calculations is significantly different than the effective VLF reflection height. [*Greifinger and Greifinger*, 1976] solved the problem of slowly varying (but not static) electromagnetic fields following a lightning stroke and found that the effective ionospheric height was well approximated by the altitude at which the local dielectric relaxation time ($\tau(h_i)$) equals the time after the lightning stroke, or $\tau(h_i) = \varepsilon_0/\sigma(h_i)$ where ε_0 is the permittivity of free space and, neglecting magnetic field effects, the conductivity σ of the ionosphere is

$$\sigma(h_i) = \frac{N_e(h_i)q^2}{m_e\nu_e(h_i)} + \frac{N_{ip}(h_i)q^2}{m_{ip}\nu_{ip}(h_i)} + \frac{N_{in}(h_i)q^2}{m_{in}\nu_{in}(h_i)} \qquad (3)$$

In this equation, $N_e(h_i)$, $N_{ip}(h_i)$, and $N_{in}(h_i)$ and are electron, positive ion, and negative ion densities, respectively, and $\nu_e(h_i)$, $\nu_{ip}(h_i)$, and $\nu_{in}(h_i)$ are the altitude-dependent electron, positive ion, and negative ion collision frequencies, respectively. The masses of electrons (m_e), average positive ions (m_{ip}), and average negative ions (m_{in}) are also needed. We assume the average mass of negative and positive ions in the ionosphere are 32 times the proton mass.

[19] This result is strictly valid for an exponentially varying ionosphere and for fairly long times (>100 ms) after the lightning stroke. For our comparison, we would like as accurate a quantitative estimate of h_i as possible at shorter times following the return stroke. To do this we use a finite difference time domain (FDTD) model to compute E_z and B_ϕ produced by a lightning stroke [*Hu and Cummer*, 2006] for a realistic electron density profile. We then use these simulated fields, known source parameters, and equation (2) to solve for the unknown h_i.

[20] We used a standard exponential nighttime electron density profile using the parameterization described by [*Bickel et al.*, 1970] with h' = 85 km and β = 0.5 km^{-1} with ion density and collision frequency profiles given by *Cummer et al.* [1998] and an essentially impulsive lightning stroke source (Gaussian pulse, duration 200 μs, channel length = 7 km) in this model. We then computed the ground level electric field waveform at ranges of 52, 70, 77, and 95 km, which correspond to the ranges of the observed signals analyzed here. About 5 ms after the lightning, at all ranges, the slow increase of the static electric field produced by the descending ionosphere [*Greifinger and Greifinger*, 1976] was evident.

[21] Figure 3 shows the resulting time variation for the effective ionosphere height for each range along with the $h_i(t)$ computed using the analytical but approximate approach of *Greifinger and Greifinger* [1976]. The general shape of the analytical and simulation-based curves are remarkably similar. However the effective ionosphere height extracted from the detailed numerical simulations is approximately 2 km lower for all ranges and times. This small discrepancy is not surprising given that the approximations made by *Greifinger and Greifinger* [1976] do not really apply to the short times after the return stroke examined here. However this 2-km difference does make a difference in the quantitative analysis to follow. Consequently, in our calculations below, we use the time varying effective ionosphere height computed from the simulated electric fields, which varies from about 68 km to 60 km, depending on the time after the lightning stroke.

4. Data Analysis

[22] Below we examine and analyze the magnetic and electric field signatures for the four identified events. The

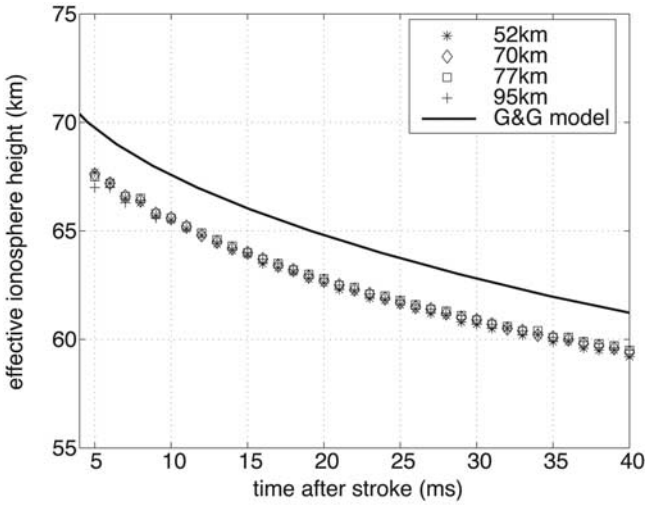

Figure 3. Effective ionosphere height versus time extracted from FDTD simulations compared with the approximate analytical approach of *Greifinger and Greifinger* [1976].

signals shown here are further low pass filtered with a 2 kHz cutoff frequency in order more clearly display the continuing current signatures without affecting the 5–10 ms time scales of interest.

4.1. 02:02:07 UT Stroke, 70.7 km Range

[23] Figure 4 shows the measured electric and magnetic fields produced by a +19.6 kA stroke that was geolocated by the NLDN to be 70.7 km from the sensors. Both signals clearly show the signature of continuing current. As noted in section 2, we focus our analysis on the time window from 10 ms after the return stroke, to ensure that a quasi-static state has been realized, to 40 ms after the return stroke, to ensure that the signals are not significantly reduced by the low end frequency response of the sensors. In this period, according to Figure 3 the effective ionospheric height drops from 66 to 59 km altitude with our assumed nighttime ionospheric conditions.

[24] Equations (1) and (2) show that while E_z is proportional to instantaneous charge moment change, B_ϕ is proportional to instantaneous current moment. Recall that the point charge approximation in these equations is reasonable for long distance measurements. Consequently, in a slowly varying continuing current signature, B_ϕ should be proportional to the time rate of change of E_z. Qualitatively, this is what Figure 4 shows; E_z is increasing but at a continuously decreasing rate, while B_ϕ is continuously decreasing.

[25] A precise quantitative analysis would account for the time variation of h_i and the slowly decaying amplitude of the continuing current. However noise and modest calibration uncertainties limit the precision of any detailed comparison to approximately 5–10%. Consequently some approximations simplify our analysis without affecting the conclusions. First, we note that the temporal average of the magnetic field signature of the continuing current is 0.24 nT over the 10 to 40 ms window of interest, while the electrostatic field change over the same period is 4.3 V/m. During this period h_i drops from 66 km to 59 km, which we average to a constant 63 km.

[26] Substituting E_z = 4.3 V/m, r = 70.7 km, h_i = 63 km, and ℓ = 7 km into equation (2) yields

$$Q_E\ell = 150\,\mathrm{C\,km}$$

for the total charge moment change produced by the continuing current from 10 to 40 ms as inferred from the electric field measurement (denoted by the E subscript).

[27] Similarly, substituting the same values but B_ϕ = 0.24 nT into equation (1) yields

$$I_B\ell = 4630\,\mathrm{A\,km}$$

for the average value of the continuing current moment during the same window. Multiplying this by the 30 ms window duration yields

$$Q_B\ell = 139\,\mathrm{C\,km}$$

for the total charge moment change produced by this continuing current as inferred from the completely independent magnetic field measurement. These values are within 8% and thus agree well given the uncertainties due to noise and sensor calibration. As noted above, it is the current and charge moments that directly drive the distant magnetic and electric fields, and thus we leave these inferred quantities in moment form.

[28] The sensitivity of the above numbers to uncertainties is small. A reduction in channel length ℓ by a factor of 2 to 3.5 km reduces $Q_E\ell$ by only 2% and $Q_B\ell$ by only 0.3%. An increase in h_i to 66 km reduces $Q_E\ell$ by only 5% and increases $Q_B\ell$ by only 2% (which, interestingly, makes them almost equal). This relatively modest sensitivity to h_i justifies our approximation of treating h_i as constant during the 30 ms window analyzed. The largest sensitivity is in $Q_E\ell$ to the distance r. If the distance is increased by 2 km to 72.7 km, then $Q_E\ell$ increases by 13% while $Q_B\ell$ increases by only 4%. This is relevant because the center of charge removal in the cloud, whose location determines E_z, may be offset from the location of the majority of the cloud-to-

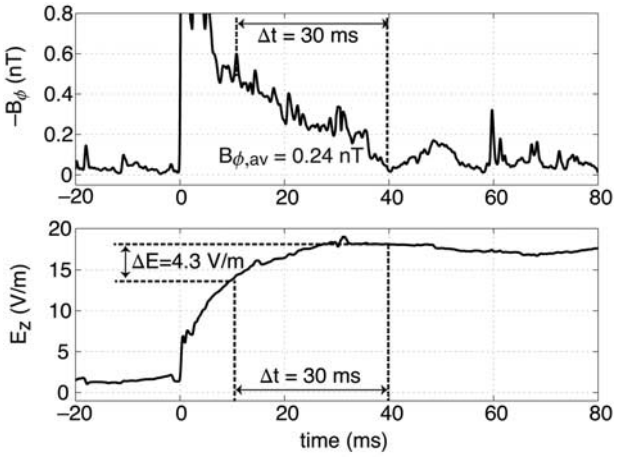

Figure 4. Measured B_ϕ and E_z versus time for a +19.6-kA stroke 70.7 km from the sensors on 15 July 2005 at 02:02:07.635 UT.

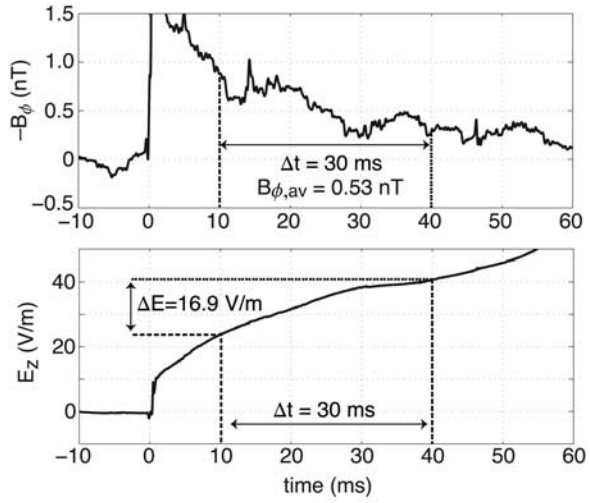

Figure 5. Measured B_ϕ and E_z versus time for a +22.8-kA stroke 52.1 km from the sensors on 15 July 2005 at 02:05:34.031 UT.

ground lightning channel, whose location determines B_ϕ [*Krehbiel et al.*, 1979]. There is no simple way of determining this offset without detailed, local measurements. Similarly, contributions to the static electric field from purely horizontal charge motion can contribute to fields at short ranges [*Krehbiel et al.*, 1979]. By choosing relatively distant strokes (50–95 km) we attempt to minimize any contributions to the field from horizontal charge motion.

[29] The good quantitative agreement we obtain for this event and those below indicates that the above uncertainties are minor and do not do not affect the conclusion that the E_z and B_ϕ continuing current signatures are quantitatively completely consistent for this event. We note in particular that the image fields partly cancel in the expression for E_z while they only add in the expression for B_ϕ. This is the physical reason for the significantly reduced sensitivity of $Q_B\ell$ to uncertain parameters, particularly the ionospheric height and the distance to the lightning. This in turn makes estimates of continuing currents from remote magnetic fields a generally more reliable technique for measuring continuing currents, provided the B_ϕ signature of continuing current can be measured with a reasonable signal to noise ratio.

4.2. The Other Three Strokes

[30] We now examine the remaining three events in the same way. Figure 5 shows the magnetic and electric fields recorded during a +22.8 kA NLDN-detected stroke on 15 July 2005 at 02:05:34.031 UT at a range of 52.1 km from the sensors. Both signals clearly show qualitatively consistent continuing current signatures in a quasi-static magnetic field and a close to linearly increasing electric field. During the same 10 to 40 ms window used above, the average magnetic field amplitude is 0.53 nT and the total electrostatic field change is 16.9 V/m. Note that the electric field change is larger relative to the magnetic field compared to the previous event, but this is expected because the fields were measured almost 20 km closer to the lightning in this case.

[31] Using these values in equations (1) and (2) with r = 52.1 km, h_i = 63 km, and ℓ = 7 km yields

$$Q_E\ell = 178\,\mathrm{C\,km}$$

$$Q_B\ell = 192\,\mathrm{C\,km}$$

for the total continuing current charge moment change in the 10 to 40 ms window as inferred from the electric and magnetic field measurements, respectively. These values are within 8% and are thus again quantitatively consistent in light of the uncertainties in this inversion.

[32] Figure 6 shows the magnetic and electric fields recorded during a +71.8 kA NLDN-detected stroke on 15 July 2005 at 03:43:10.870 UT at a range of 95.8 km from the sensors. Both signals again clearly show qualitatively consistent continuing current signatures in a quasi-static magnetic field and a close to linearly increasing electric field. During the 10 to 40 ms window, the average magnetic field amplitude is 0.73 nT and the total electrostatic field change is 3.0 V/m. Note that the electric field change is much smaller relative to the magnetic field compared to the previous two events. This is because the fields were measured 25 km and 45 km farther away from the lightning, almost at the maximum range where an electrostatic signature is detectable. These signals exhibit a minor discrepancy in that the time of zero E_z slope is slightly offset from the time of zero B_ϕ, but this is not surprising as neither signal is noise-free.

[33] Using these values in equations (1) and (2) with r = 95.8 km, h_i = 63 km, and ℓ = 7 km yields

$$Q_E\ell = 447\,\mathrm{C\,km}$$

$$Q_B\ell = 630\,\mathrm{C\,km}$$

for the total continuing current charge moment change in the 10 to 40 ms window as inferred from the electric and magnetic field measurements, respectively. The 41%

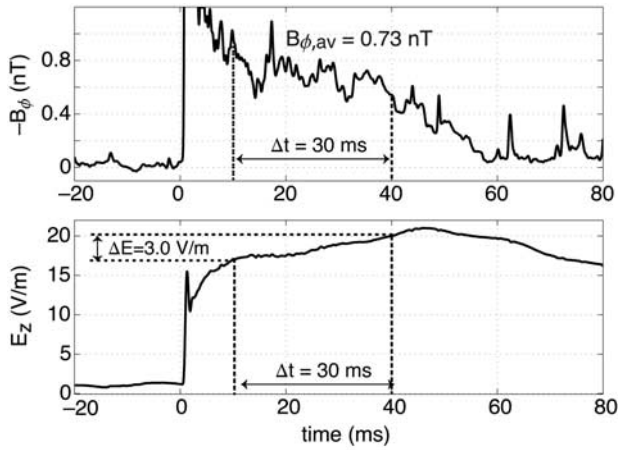

Figure 6. Measured B_ϕ and E_z versus time for a +71.8-kA stroke 95.8 km from the sensors on 15 July 2005 at 03:43:10.870 UT.

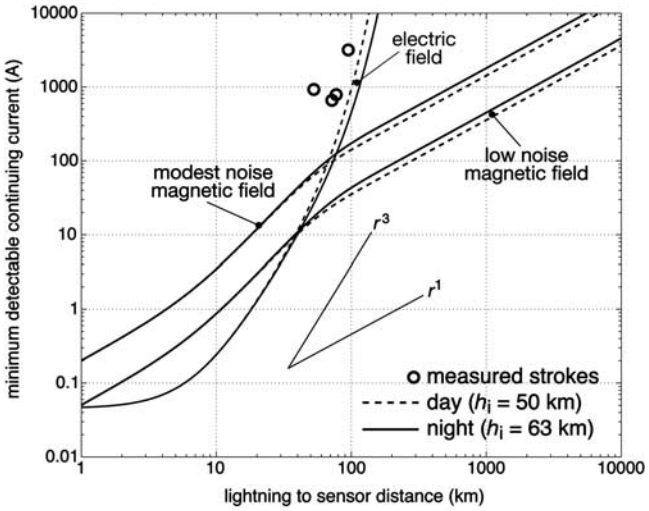

Figure 7. Minimum detectable continuing current for different sensors vs. distance to sensor. Plotted for reference are r^3 and r^1 lines, and the circles show the measured continuing current and range for the 4 events analyzed here.

disagreement is significantly bigger than in the other two cases. This is not surprising for several reasons. This is the smallest analyzed electric field change and thus is most susceptible to noise. There is some evidence of this possibility. The magnetic field continuing current signature is clear until at least 60 ms after the return stroke, yet the electric field slope changes sign after 45 ms, indicating that local effects may have reduced the measured electrostatic field change. If the measured E_z were increased just to 4.2 V/m, the values would be almost identical. Also, at this long range, the electrostatic field change is a very strong function of distance. If the range from the centroid of cloud-altitude charge removal were 101.8 km instead of the assumed 95.8 km, the electric field inferred charge moment change would increase to 624 C km. A modest 6 km offset between the cloud to ground channel and the centroid of charge removal is not unreasonable for a large positive CG stroke.

[34] Although the quantitative agreement is not as good as for the other two events, the long range for this event substantially increases the uncertainties in the inversion. And, despite these uncertainties, the electric and magnetic field signatures for this event both show continuing current charge moment changes of approximately 500–600 C km. This continues to demonstrate that the magnetic and electric field signatures are both produced by the same continuing current.

[35] The last of the four analyzed events is very similar to the first and we thus do not show the data in a figure. This was a +22.5 kA NLDN-detected stroke on 15 July 2005 at 02:13:06.563 UT at a range of 77.5 km from the sensors. During the 10 to 40 ms window the average magnetic field was 0.24 nT and the electric field change was 3.4 V/m. This yields $Q_E\ell$ = 178 C km and $Q_B\ell$ = 158 C km, for agreement within 13%. Once again, the observed electrostatic field change and quasi-static magnetic field are quantitatively consistent as being produced by the same magnitude continuing current. Taken together, these four events confirm that continuing currents can be reliably detected and measured at long ranges using their magnetostatic signature.

4.3. Detection Range Estimates

[36] There are practical differences in how well continuing currents can be measured using the electrostatic and magnetostatic signatures. Electric field sensors are relatively simple to build and over some ranges the signals of interest are large. However the electrostatic field signature falls as approximately r^{-3} at ranges more than a few tens of km, and only very large continuing currents can be detected as far as 100 km, as we showed for one event above. Additionally, at close ranges, electrostatic signals from in-cloud charge motion can be large *Krehbiel et al.* [1979] and it is nearly impossible to distinguish these from continuing current signatures.

[37] In contrast, the constructive interference between vertical image currents yields a magnetostatic field that decays approximately as r^{-1} at long ranges from the source [*Cummer and Füllekrug*, 2001]. This means that the detection range can be much longer using magnetic field measurements. The main challenge in using the magnetic signature is that the signals are typically small (a fraction of a nT) and slowly varying. Most types of DC magnetometers lack the sensitivity for this measurement, and coil-based AC magnetometers must be carefully designed to have sufficient sensitivity at the low frequencies needed (several Hz).

[38] Using the data presented here we can quantitatively compare the typical detection and measurement range for electric and magnetic field sensors. At the Colorado sensor location where the data reported here were recorded, a quasi-static magnetic field signature can be discerned and measured if it exceeds approximately 40 pT in amplitude. At this location the noise is site limited, not sensor limited. At a lower noise Duke University site, similar sensors yield a detection sensitivity of approximately 10 pT. Using equation (1), we use these noise limits to estimate the minimum magnetic field detectable continuing current (assuming a 7 km channel length) as a function of range. This minimum detectable continuing current for low and modest noise sensor sites is shown in Figure 7.

[39] Similarly, the electric fields measured at the YRFS location indicate a minimum detectable electrostatic field slope of approximately 0.5 V/m across the 30 ms windows examined here. Smaller static field slopes would be difficult to discriminate from other background signals produced by other storm-related processes. Using equation (2), this noise limit yields the minimum electric field detectable continuing current (again assuming a 7 km channel length) as a function of range, which is also shown in Figure 7.

[40] As expected, an electric field sensor is better at detecting continuing currents at short ranges because of the strength of the electrostatic signal. Depending on the noise, a magnetic field sensor becomes more sensitive at ranges beyond 40–70 km. Importantly, the slow r^{-1} decay of the magnetic field signal with distance means that the minimum detectable continuing current increases only linearly with distance. Thus modest to large continuing currents can be detected at rather large ranges with a sufficiently sensitive magnetic field sensor. For example, at a low noise site, a 1000 A continuing current is detectable

to a range of 3000 km. Note that this magnitude and range is essentially what was demonstrated by *Cummer and Füllekrug* [2001]. Even a modest continuing current of several hundred amps is detectable out to almost 1000 km range with commercially available sensors placed at a low noise site.

[41] The four measured continuing currents and detection ranges are also plotted in the figure. The data points fall in the range where the electric and magnetic field detection sensitivities are comparable, and this is reflected in the comparable ease of visually identifying the continuing current signatures in the electric and magnetic field waveforms shown in Figures 3–5. The magnetic field signal appears noisier because it is approximately the time derivative of the electric field signal.

5. Conclusions

[42] We have shown that presumed electric and magnetic signatures of lightning continuing current are quantitatively consistent. Using simultaneously recorded signatures from 4 separate lightning strokes, we separately computed from the vertical electric field and the azimuthal magnetic field the total charge moment changes produced by the continuing current in a 30 ms time window based on electro- and magnetostatic approaches. For 3 events between 52 and 77 km from the sensors, these independent values agreed to within better than 13%. We demonstrated that discrepancies of this magnitude are attributable to instrument calibration uncertainties and in imperfectly known numerical parameters such as the effective ionospheric height. The fourth event exhibited a larger difference of 41%, but the long distance (96 km) of this event creates very significant uncertainties related to the precise distance between the centroid of charge removal and the sensor. Collectively, these events conclusively show that the quasi-static magnetic signature previously attributed to continuing lightning currents [*Cummer and Füllekrug*, 2001] is, in fact, produced by continuing currents.

[43] Because of the way that ground and ionospheric image charges and currents contribute to distant fields, the magnetic field signature of continuing current is less distance-dependent than the corresponding electric field signature. Using realistic noise thresholds established by the measured signals presented here, we estimated the minimum detectable continuing current amplitude as a function of range for magnetic and electric field sensors. The magnitude of the electrostatic signature at ranges less than a few tens of km makes an electric field more sensitive for short ranges, although small continuing currents (tens of amps) can also be magnetically detected at these ranges. However the range of detectability for magnetic field sensors far exceeds that for electric field sensors. Using high sensitivity magnetic sensors at a low noise site, modest continuing currents of several hundred amps are detectable as far away as 1000 km.

[44] **Acknowledgments.** This research was supported by NSF Dynamic and Physical Meteorology Program grant ATM-0642757 to Duke University. We thank Dr. Walt Lyons for hosting and helping to support our instrumentation at the Yucca Ridge Field Station during the summer of 2005.

References

Bickel, J. E., J. A. Ferguson, and G. V. Stanley (1970), Experimental observation of magnetic field effects on VLF propagation at night, *Radio Sci.*, *5*, 19–25.

Brook, M., N. Kitagawa, and E. J. Workman (1962), Quantitative study of strokes and continuing currents in lightning discharges to ground, *J. Geophys. Res.*, *67*, 649–659.

Cummer, S. A., and M. Füllekrug (2001), Unusually intense continuing current in lightning causes delayed mesospheric breakdown, *Geophys. Res. Lett.*, *28*, 495–498.

Cummer, S. A., U. S. Inan, and T. F. Bell (1998), Ionospheric D region remote sensing using VLF radio atmospherics, *Radio Sci.*, *33*, 1781–1792.

Cummins, K. L., M. J. Murphy, E. A. Bardo, W. L. Hiscox, R. B. Pyle, and A. E. Pifer (1998), A combined TOA/MDF technology upgrade of the US National Lightning Detection Network, *J. Geophys. Res.*, *103*, 9035–9044.

Fisher, F. A., and J. A. Plumer (1977), Lightning protection of aircraft, technical report, NASA Ref. Publ., NASA-RP-1008, NASA Lewis Research Center.

Fisher, R. J., G. H. Schnetzer, R. Thottappillil, V. A. Rakov, M. A. Uman, and J. D. Goldberg (1993), Parameters of triggered-lightning flashes in Florida and Alabama, *J. Geophys. Res.*, *98*, 22,887–22,902.

Fuquay, D. M., R. G. Baughman, A. R. Taylor, and R. G. Hawe (1967), Characteristics of seven lightning discharges that caused forest fires, *J. Geophys. Res.*, *72*, 6371–6373.

Greifinger, C., and P. Greifinger (1976), Transient ULF electric and magnetic fields following a lightning discharge, *J. Geophys. Res.*, *81*, 2237–2247.

Hu, W., and S. A. Cummer (2006), An FDTD model for low and high altitude lightning-generated EM fields, *IEEE Trans. Antennas Propag.*, *54*, 1513–1522.

Krehbiel, P. R., M. Brook, and R. A. McCrory (1979), An analysis of the charge structure of lightning discharges to ground, *J. Geophys. Res.*, *84*, 2432–2456.

Nakahori, K., T. Egawa, and H. Mitani (1982), Characteristics of winter lightning currents in Hokuriku district, *IEEE Trans. Power Appar. Sys.*, *101*, 4407–4412.

Rakov, V. A., and M. A. Uman (2003), *Lightning*, Cambridge Univ. Press, Cambridge, UK.

Shindo, T., and M. A. Uman (1989), Continuing current in negative cloud-to-ground lightning, *J. Geophys. Res.*, *94*, 5189–5198.

Williams, D. P., and M. Brook (1963), Magnetic measurements of thunderstorm currents, *J. Geophys. Res.*, *68*, 3243–3247.

S. A. Cummer, Electrical and Computer Engineering Department, Duke University, Box 90291, Durham, NC 27708, USA. (cummer@ee.duke.edu)

T. K. Nielsen and Y. Zhang, QUASAR Federal Systems, Inc, 5754 Pacific Center Blvd., Suite 203, San Diego, CA 92121, USA.

M. Ross, MTS Systems Corporation, 3001 Sheldon Dr, Cary, NC 27513 USA.